Journal of the European Ceramic Society 19 (1999) 543–552

PII: S0955-2219(98)00251-9
0955-2219/99/$—see front matter

$\alpha \rightarrow \beta$ Sialon Transformation in Calcium-containing α-SiAlON Ceramics

Hasan Mandal[a] and Derek P. Thompson[b]*

[a]Department of Ceramics Engineering, Anadolu University, 26470, Eskisehir, Turkey
[b]Materials Division, Department of Mechanical, Materials and Manufacturing Engineering, Newcastle University, Newcastle, NE1 7RU, UK

(Received 6 March 1998; revised version received 24 September 1998; accepted 30 September 1998)

Abstract

Recent studies on rare earth densified α-sialon ceramics have shown that the resulting α-sialon product, present either as a single phase or in conjunction with β-sialon, is unstable when heat treated at lower (1350–1600°C) temperatures, and transforms to a mixture of β-sialon plus other crystalline or liquid metal sialon phases. The present paper describes similar studies carried out on calcium-densified α-sialon compositions, and shows that for a wide range of starting compositions, with calcium as the sole sintering additive or present with other (Nd, Sr) cations, the resulting calcium stabilised a-sialon products are fully resistant towards α→β transformation when heat treated in the temperature range 1450–1550°C. Whereas α→β transformation in rare earth stabilised α-sialons is influenced by the nature of the rare earth cation, the α-sialon composition, the composition and melting behaviour of the liquid phase and the presence or absence of β-sialon nuclei, transformation in calcium a-sialons appears to be influenced by none of these parameters. Clearly if α→β sialon transformation occurs in this system, the transformation temperature for calcium α-sialons must be below 1450°C, the heat-treatment temperature which has been most frequently used in current research on rare earth densified α-sialons. © *1999 Published by Elsevier Science Limited. All rights reserved*

Keywords: sialon, transformation, microstructure—final, alkaline earth oxides, electron microscopy.

*To whom correspondence should be addressed. Fax: +44 0191 222 7153; e-mail: d.p.thompson@ncl.ac.uk

1 Introduction

Si_3N_4 based ceramics are attractive materials for high temperature and wear resistant applications. However, they are difficult to density without sintering additives because of the covalent nature of the bonding and the very low self-diffusion coefficients of the atoms involved. Therefore metal oxides are necessary for densification, and during sintering, the metal oxide additives and silicon nitride (including a small amount of silica), form a eutectic melt which aids densification.

Pressureless sintered β-sialons of general composition, $Si_{6-z}Al_zO_zN_{8-z}$ (where $z \leq 4{\cdot}0$) were the first nitrogen ceramics to achieve large scale commercial viability. This was because the presence of alumina in the starting mix lowers the eutectic temperature of the densifying liquid by ~-200–300°C, making it possible to achieve full density by pressureless sintering. The resulting β-sialon materials have Young's moduli of $\approx$300 GPa, strengths of up to 1000 MPa and K_{IC} values of up to 8 $MPam^{1/2}$ at room temperature. The liquid phase, however, remains as a grain boundary glass after sintering which degrades high temperature properties in subsequent use.

α-Sialon, unlike β-sialon, can accommodate additional cations into its structure because the unit cell contains two large interstices. The general formula is $M_xSi_{12-(m+n)}Al_{(m+n)}O_nN_{(16-n)}$ where $x < 2$ and M is Li, Mg, Ca, Y and Ln $\geq$58. An important advantage of α-sialons is that the amount of intergranular phase is reduced by the transient liquid phase being absorbed into the matrix α-sialon phase during sintering. Another advantage is that the final product shows increased hardness.

α and β-Sialon phases are completely compatible and α-sialon/β-sialon composites are readily prepared by a single stage sintering of appropriate

mixes of nitrides and oxides. Therefore, in recent years, mixed $\alpha-\beta$ sialon materials have received increasing attention because of their easier fabrication compared with Si_3N_4 ceramics, and more importantly because the mechanical properties can be optimized because of the high hardness of α-sialon and the good strength and toughness of β-sialon.[1,2]

Recently, it has been found that the phase composition and microstructure of $\alpha-\beta$ sialon ceramics is greatly affected by heat treatment procedures when rare earth oxides are used as the sintering additive.[3–5] The α-sialon phase is only stable at high ($\geq$1650°C) temperatures and transforms to rare earth rich intergranular phases plus β-sialon when heat-treated at lower temperatures, this provides a convenient mechanism for controlling the mechanical properties of the final material. However, this transformation can only be used beneficially in applications where the maximum service temperature is below the transformation temperature of the grain boundary glass (1000°C). High temperature properties, especially oxidation and creep resistance, significantly deteriorate above this temperature because of the residual glass.

Our previous work and research in other laboratories has concentrated on achieving an understanding of the mechanism of $\alpha\rightarrow\beta$ sialon transformation.[6–13] A combination of X-ray and microstructural observations on sintered and heat-treated rare earth densified mixed $\alpha-\beta$ sialon and α-sialon ceramic composites has shown that the amount and composition of liquid phase, type of sintering additive, heat treatment temperature and time, type of crystalline grain boundary phases and the presence of β-sialon grains are all important factors which affect the transformation. However, a full understanding of the transformation mechanism is still not available.

Most of the present work has focused on rare-earth densified α-sialons, and these all show a tendancy to transform to β-sialon when heat-treated at lower temperatures. However, recent work in the calcium sialon system, has shown that calcium α-sialons not only exhibit a much larger stability field than rare earth α-sialons, but also are much more resistant towards $\alpha\rightarrow\beta$ transformation.[14] It is clear that more information can be gleaned about the transformation by studying calcium and mixed calcium/rare-earth α-sialons. In the present work, α-sialon and mixed $\alpha-\beta$ sialon starting compositions have therefore been densified by hot pressing using CaO, SrO, Yb_2O_3, Nd_2O_3 and mixed Yb–Ca, Ca–Nd and Ca–Sr oxides. The resulting materials have been heat-treated at 1450°C for up to 1 month to observe $\alpha\rightarrow\beta$ sialon transformation behaviour. The effects of different cation size, cation valency, heat treatment time, composition and the presence of β-sialon grains are discussed.

2 Experimental

The overall compositions of the prepared starting powder mixtures corresponded to single-phase α-sialons with $m = 1{\cdot}5$ and $n = 1{\cdot}5$. These were prepared by using Si_3N_4, AlN, Al_2O_3 together with M_xO_y (M = Ca, Sr, Nd, Yb or mixtures i.e. Ca–Sr, Ca–Nd, Yb–Nd). The source materials used were silicon nitride (HC Starck Grade LC10), aluminium nitride (HC Starck-Berlin, Grade A) and aluminum oxide (Sigma Chemical Company Ltd). The added metal oxides were calcined at 800°C for 4 h before use, to remove absorbed water. When calculating the compositions, 3·5% SiO_2 and 3·5% Al_2O_3 (the manufacturer's specifications) present on the surfaces of Si_3N_4 and AlN, respectively, were taken in account.

The starting powders were mixed in water-free isopropanol and milled in an agate mortar for 45 min. The size of batch used was 15 g. After drying and sieving, powders were compacted into pellets (about 3 g) by uniaxial and then isostatic pressing at 200 MPa. The green pellets were hot pressed in BN-coated graphite dies at 180°C for 1 h. All sintered materials were placed in a carbon crucible and re-heated up to 180°C in a smaller size pressureless sintering furnace for 20 min and quenched (400°C min^{-1}) to room temperature. Heat treatment was carried out on all samples in an alumina tube furnace at 1450°C for up to 720 h (1 month) in a nitrogen gas atmosphere.

Product phases were characterised by X-ray diffraction (XRD) using a Hägg-Guinier camera and CuKα_1 radiation. A computer linked line scanner system (Type SCANPI LS-20) developed by Werner (Arrhenius Laboratory, Stockholm University) was used for direct measurements of X-ray films and refinement of lattice parameters. The amounts of α and β-sialon phases were found by quantitative estimation from the XRD pattern using the integrated intensifies of the (102) and (210) reflections of α-sialon and the (101) and (210) reflections of β-sialon.[15] The curves used were originally developed for α-Si_3N_4 rather than α-sialon, and therefore the amounts of α-sialon reported in this paper are overestimated by up to 10% compared with their true values because of the increased intensifies of α-sialon lines for a given amount of sample compared with α-Si_3N_4 values.

After application of a conducting coating (gold for microstructural examination and carbon for EDX work), polished surfaces of as-sintered and heat treated samples were examined using a Camscan S4-80 DV scanning electron microscope (SEM)

equipped with EDX facilities and a windowless detector suitable for light element analysis.

3 Results

The $m = 1{\cdot}5$, $n = 1{\cdot}5$ composition was selected for study because this is close to the minimum oxygen limit of α-sialon compositions for easy investigation (i.e. excluding the use of metal nitrides as starting compounds because of their expense and sensitivity to hydrolysis). Also a recent study has focused on these compositions for a range of rare earth α-sialons.[10,11]

Table 1 gives densities of various samples after sintering under different conditions. Examination of polished cross-sections of the hot-pressed sialon ceramics by SEM showed only a few micro-pores to be present, indicating that samples were essentially of theoretical density after hot-pressing.

The relative amounts of α and β sialon phases after sintering were established by XRD and are shown in Table 2. As seen from the table, 100% of α-sialon, as anticipated, was obtained for the sintering additives CaO, Yb_2O_3 and the mixed oxides of Nd/Yb, Nd/Ca and Sr/Ca. Minor amounts of 21R polytypoid and M′ phases appeared in the Nd, Nd–Yb and Nd–Ca α-sialon compositions. Although α-sialon was still the predominant phase when Nd_2O_3 was used as the sintering additive, some 3% of β-sialon was also observed. The increasing α-sialon phase homogeneity limits (m and n values) with increasing Z and decreasing ionic radius have been established in previous work on rare earth sintering additives.[16]

Although the cation size of Ca (0·99Å) is the same as Nd (0·995Å) and the mean size of Ca–Sr (1·06Å) is even larger, the Ca, Ca–Nd and Ca–Sr densified samples produced pure α-sialon. This difference can be explained in terms of lower valency of Ca (+2), since α-sialon stability increases with increasing cation solubility x (where $x = m/v$, and v is the cation valency), which in turn increases with decreasing cation valency.

In the case of SrO additions, no α-sialon phase was observed since the cation size of Sr is too large. (1·12Å). The sintered material contained only β-sialon and a significant amount of the phase, S ($SrO1{\cdot}3Al_2O_30{\cdot}7Si_2N_2O$), which has the same X-ray diffraction pattern reported by Hwang *et al.*[17]

Back-scattered scanning electron micrographs were examined on polished sections of sintered specimens after rapid cooling (see Fig. 1). Because of the large atomic numbers of rare earth elements, it is very easy to clearly distinguish between the various phases present. The β-sialon and 21R grains (which contain no sintering additive cation) are black and more needlelike, whereas the α-sialon grains (which contain a small amount of sintering additive cation) are grey and more equiaxed whilst the rare earth cation rich crystalline or glassy phases appear fine grained and white, because of the high rare earth content. Since the atomic number

Table 1. Densities of samples hot-pressed at 1800°C

Sample code	*Sintering additive(s)*	*Intended final phase assemblage*	*Density (g cm^{-3})*
HM1	CaO	100% α-sialon	3·200
HM2	Yb_2O_3	100% α-sialon	3·543
HM3	Nd_2O_3	100% α-sialon	3·445
HM4	SrO	100% α-sialon	3·420
HM5	Nd_2O_3–CaO	100% α-sialon	3·350
HM6	SrO–CaO	100% α-sialon	3·260
HM7	Yb_2O_3–Nd_2O_3	100% α-sialon	3·520
HM8	CaO	90% α–10% β sialon	3·210
HM9	CaO	50% α–50% β sialon	3·190
HM10	CaO	55% α–35% β-10% glass	3·130

Table 2. X-ray results of sintered and fast cooled samples

Sample	α-*Sialon (%)*	β-*Sialon (%)*	*Other(s)*
HM1	vs (100)	—	—
HM2	vs (100)	—	—
HM3	vs (97)	vw (3)	21R (w)
HM4	mw (12 α-Si_3N_4)	s (88)	S(m)
HM5	vs (100)	—	21R(vw)
HM6	vs (100)	—	α-Si_3N_4(w)
HM7	vs (100)	—	21R(w)
HM8	vs (100)	—	—
HM9	vs (93)	w (7)	—
HM10	s (90)	mw (10)	Geh (w)

Note: for X-ray intensifies, s = strong, m = medium, w = weak, v = very; numbers in parentheses are relative percentages of α- and β-sialon phases, 21R = sialon polytypoid. S = ($SrO1{\cdot}3Al_2O_30{\cdot}7Si_2N_2O$), Geh = $Ca_2Al_2SiO_7$.

of Ca (20) is much less than the rare earths (57–72), EDX analysis cannot as easily distinguish between the different phases in the same way. Thus in all the pure calcium sialon samples examined here, it was impossible to distinguish α-, β- and glassy phases in the way outlined above, and in Fig. 1(a), despite the 100% α-sialon XRD result, it is expected that small pockets of residual glass will remain, but any contrast from these regions because of the increased calcium content is not sufficient to be observed. In a similar way, Samples HM9 and HM10 looked identical to HM1, because the β grains (plus any residual glass) did not show up in back-scattered mode.

Micrographs of the Ca–Nd sample [Fig. 1(d)] do show some contrast, and three phases are clearly apparent. Since calcium alone does not give this contrast, this provides clear evidence that Nd must be present in both the glass (white dots) and the α-sialon grains which make up most of the microstructure. This conclusion is also supported by the unit cell data in Table 3. From the mixed Nd/Yb sample [Fig. 1(e)], it is impossible from the micrograph alone to say whether both Nd and Yb are present in the α-sialon phase as suggested by the EDX spectrum [Fig. 2(b)]. The unit cell dimensions in Table 3 would suggest that Nd is the dominant cation in the α-sialon phase. The S-phase in the

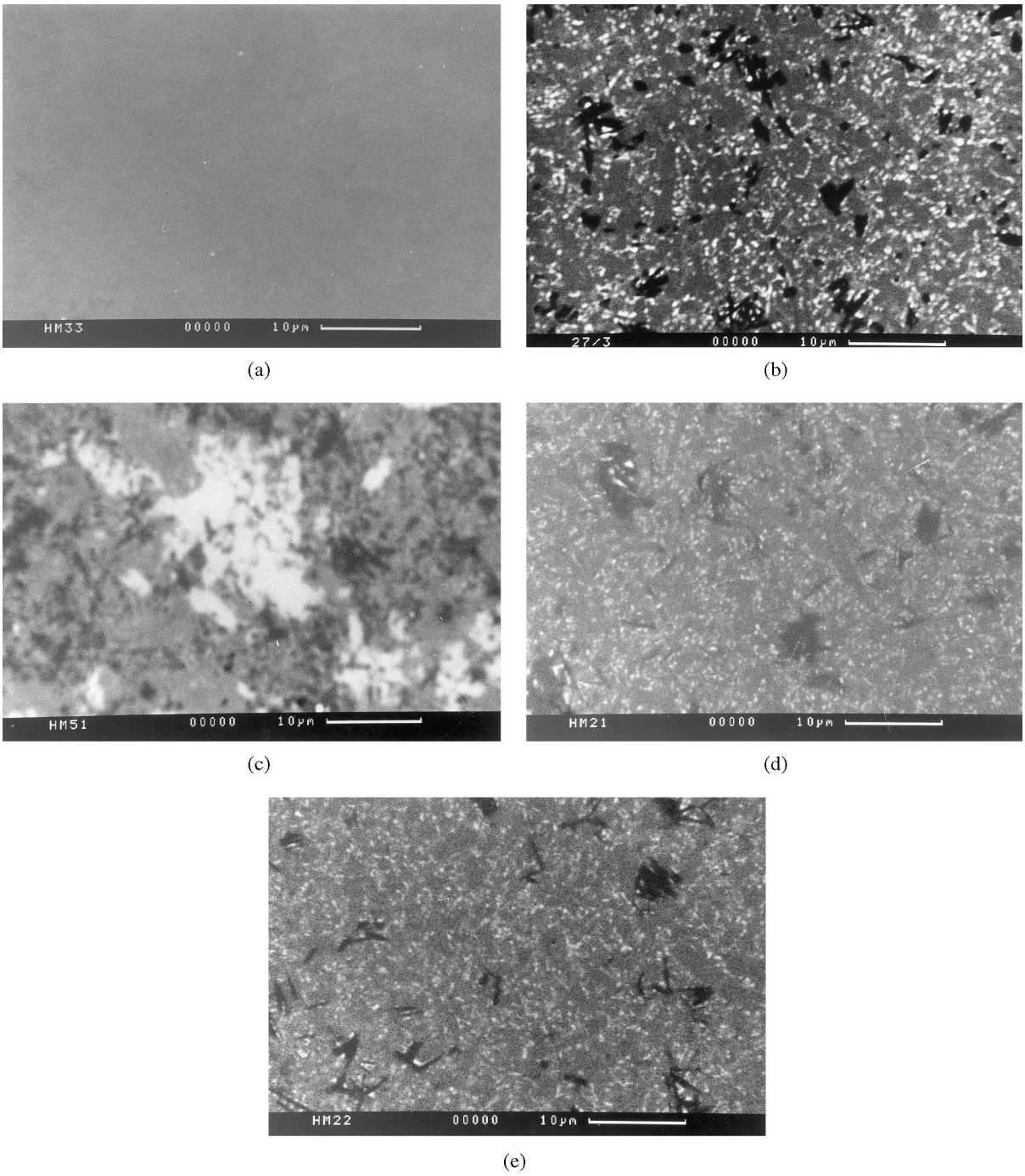

Fig. 1. Back-scattered SEM micrographs of the (a) CaO, (b) Nd_2O_3, (C) SrO, (d)Nd_2O_3CaO, (e) Nd_2O_3–Yb_2O_3 samples after fast cooling.

Sr-containing sample, HM4, is clearly apparent as clumps of whitish grains in the microstructure [Fig. 1(c)].

Results of prolonged heat treatment for up to 720 h (1 month) at 1450°C are given in Table 4. As can be seen from the table, with the exception of pure Nd_2O_3, no $\alpha \rightarrow \beta$ sialon transformation was observed for most of the other sintering additives. In the heat treated Nd_2O_3 sample, the amount of α-sialon gradually decreased as the heat treatment time increased and no α-sialon remained after 720 h at 1450°C. An increased amount of M′-phase

Table 3. As hot-pressed α-sialon unit cell dimensions

Sample code	*Sintering additive*	*Unit cell dimensions (Å)*	
		a	c
HM1	CaO	7·84667	5·70554
HM2	Yb_2O_3	7·81950	5·69800
HM3	Nd_2O_3	7·81550	5·69300
HM4	SrO	No α-sialon	
HM5	Nd_2O_3–CaO	7·83331	5·70091
HM6	SrO–CaO	7·82056	5·68923
HM7	Yb_2O_3–Nd_2O_3	7·82013	5·69848
HM8	CaO	7·83851	5·70441
HM9	CaO	7·81278	5·68691
HM10	CaO	7·81155	5·68557

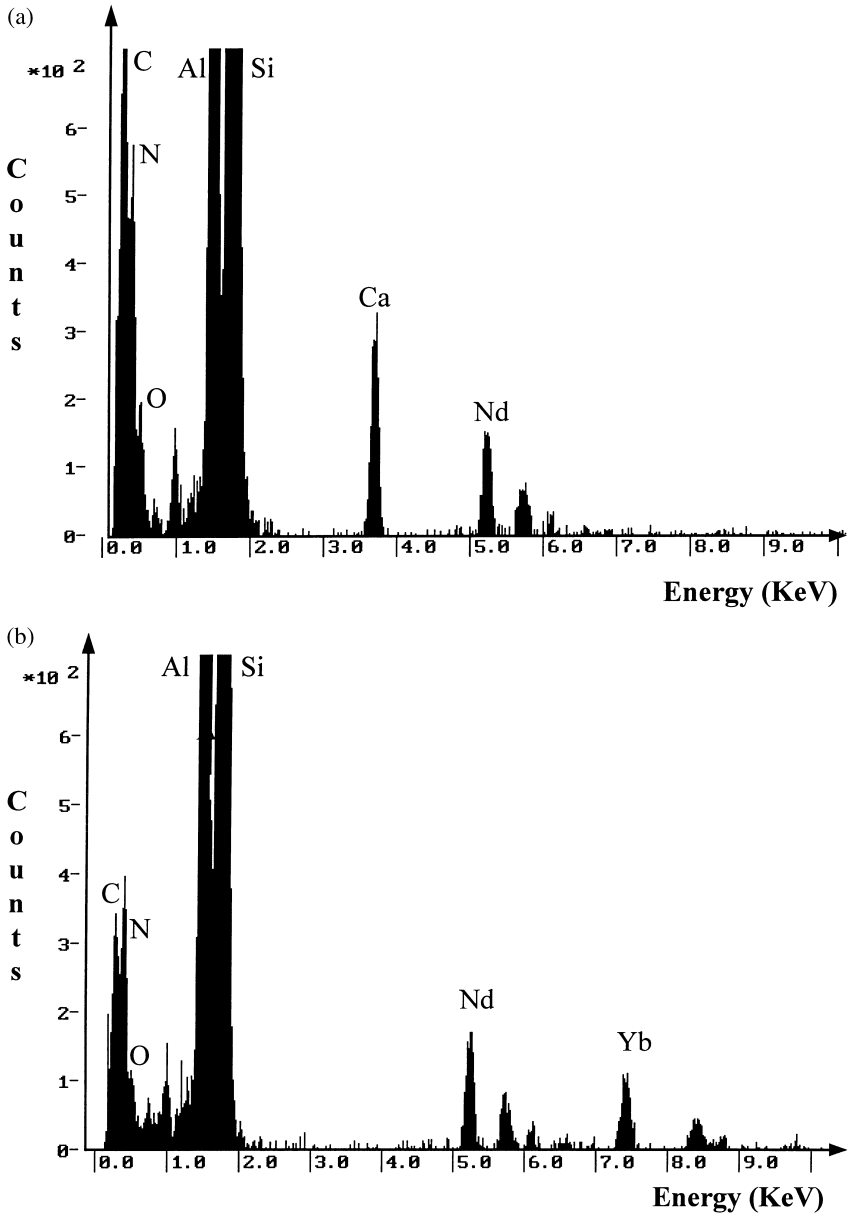

Fig. 2. EDX spectra of the α-sialon regions of (a) CaO– Nd_2O_3, (b) Yb_2O_3–Nd_2O_3 samples after fast cooling.

formed as $\alpha \rightarrow \beta$ sialon transformation proceeded. The equation for this reaction is:

$$\alpha\text{-sialon} + \beta\text{-sialon} + 21\text{R} + \text{liquid}(1) \rightarrow \beta\text{-sialon} + 21\text{R} + \text{M}' + \text{liquid}\ (2) \quad (1)$$

α-sialon was the only matrix phase observed after 1 month of heat treatment when Yb_2O_3, CaO and mixed cations were used as additives. In addition J + garnet for Yb_2O_3, M′ for Nd–Ca and Nd–Yb and S phase for Ca–Sr additions were observed in increasing amounts along with a decrease in the α-sialon unit cell dimensions as the heat treatment temperature increased. The equation for this reaction is:

$$\alpha_1\text{-sialon} + (21\text{R}) + \text{Liquid(l)} \rightarrow \alpha_2 - \text{sialon} + 21\text{R} + \text{crystalline phase(s)(M}' \text{ or J + G or S)} + \text{Liquid(2)} \quad (2)$$

Figure 3 shows typical back-scattered SEM images of the heat treated samples after 168 h of heat treatment. These were very similar to the sintered samples except for pure Nd–, which was completely transformed to β-sialon + Nt'.

Figure 4 shows EDX spectra for heat treated Nd–Ca, Nd–Yb and Sr–Ca samples after 168 h of heat treatment, Nd– and Sr– cations still remain inside the cc-sialon grains.

It is very surprising that Nd, a low Z, large radius cation, can form a more stable α-sialon phase when present with Yb and Ca. Also Sr^{2+} ($r = 1{\cdot}12$Å) does not form an α-sialon on its own but can produce a very stable mixed-cation α-sialon phase when present along with Ca. This suggests that the $\alpha \rightarrow \beta$ sialon transformation temperature for Yb and Ca α-sialons might be much lower than 1450°C.

Previous work [10,11] has clearly shown that β-sialon grains play a key role in promoting $\alpha \rightarrow \beta$ transformation especially for small cation size sintering additives. To explore this, 10 and 50% β-of sialon powder with a z value of 0·8 (i.e. $Si_{5\cdot2}Al_{0\cdot8}O_{0\cdot8}N_{7\cdot2}$) was added to the Ca $m = 1{\cdot}5$, $n = 1{\cdot}5$ starting mix and material prepared in exactly the same way as described in Section 2. X-ray results for sintered samples showed that only 7% β-sialon was observed for the 50% β-sialon addition and no β-sialon was observed for the 10% β-sialon addition. The reason for this behaviour can be explained in terms of the larger α-sialon

Table 4. X-ray results of heat treated samples

Sample	*HT Time (h)*	*α-sialon*	*β-sialon*	*Other(s)*
HM1	24	vs(100)	—	
	168	vs(100)	—	
	720	vs(100)	—	
HM2	24	vs(100)	—	G(vvw), J(vw)
	168	vs(100)	—	G(vw), J(w)
	720	vs(100)	—	G(mw), J(mw)
HM3	24	vs(81)	mw(19)	21R(w), M′(w)
	168	vs(8)	vs(92)	21R(mw), M′(mw)
	720	–	vs(100)	21R(mw), M′(m)
HM4	24	12(α-Si_3N_4)	s(88)	S(m)
	168	12(α-Si_3N_4)	s(88)	S(m)
	720	10(α-Si_3N_4)	vs(90)	S(ms)
HM5	24	vs(100)	—	21R(vw),m′(vvw)
	168	vs(100)	—	21R(w), m′(vw)
	720	vs(100)	—	21R(w), m′(w)
HM6	24	vs(100)	—	α-Si_3N_4(vw),S(vw)
	168	vs(100)	—	α-Si_3N_4(vvw),S(vw)
	720	vs(100)	—	S(w)
HM7	24	vs(100)	—	21R(w), M′(vw)
	168	vs(100)	—	21R(w), M′(w)
	720	vs(100)	—	21R(mw), M′(m)
HM8	24	vs(100)	—	—
	168	vs(100)	—	—
	720	vs(100)	—	—
HM9	24	vs(93)	w(7)	—
	168	vs(93)	w(7)	—
	720	vs(93)	w(7)	—
HM10	24	vs(90)	mw(10)	geh(w)
	168	vs(90)	mw(10)	geh(w)
	720	vs(90)	mw(10)	geh(mw)

Note: for X-ray intensities, s = strong, m = medium, w = weak, v = very, numbers in parentheses are relative percentages of α- and β-sialon phases, 21R = sialon polytypoid; M′ = N-melilite solid solution ($Ln_2Si_{3-x}Al_xO_{3+x}N_{4-x}$); S ($SrO1{\cdot}3A1_2O_30{\cdot}7Si_2N_2O$), Geh = ($Ca_2Al_2SiO_7$); G = ($Ln_3Al_5O_{12}$); J = ($Ln_4Si_2O_7N_2$).

stability region in the Ca system. Even after 720 h of heat treatment, no change was observed in the amounts of matrix phases.

In our previous work, it was also shown that the amount and composition of the liquid phase is important in influencing $\alpha \rightarrow \beta$ sialon transformation, especially if β-sialon nucleating sites are present. To explore this effect, 10% of glass (of composition $Ca_{1\cdot875}Si_{1\cdot875}Al_{1\cdot25}O_6N$ [18]) was added to a starting composition consisting of 55% Ca α-sialon and 35% of β-sialon. The X-ray results for the sintered sample showed that only 10% of β-sialon was present and this amount did not change with heat treatment at 1450°C even after 720 h.

4 Discussion

Many of the results obtained in the present study are different from those obtained for rare earth stabilised α-sialon materials. It is clear that calcium-based α-sialons in which calcium is either the sole interstitial cation, or is present jointly with others, do not undergo $\alpha \rightarrow \beta$ sialon transformation when heat-treated at temperatures in the range 1450°C. This conclusion is true for a range of m ($0\cdot5 < m < 2\cdot0$) and n ($1\cdot0 < n < 2\cdot0$) values, and confirms the improved thermal stability of calcium α-sialons compared with rare earth analogues, and probably also correlates with the increased size of

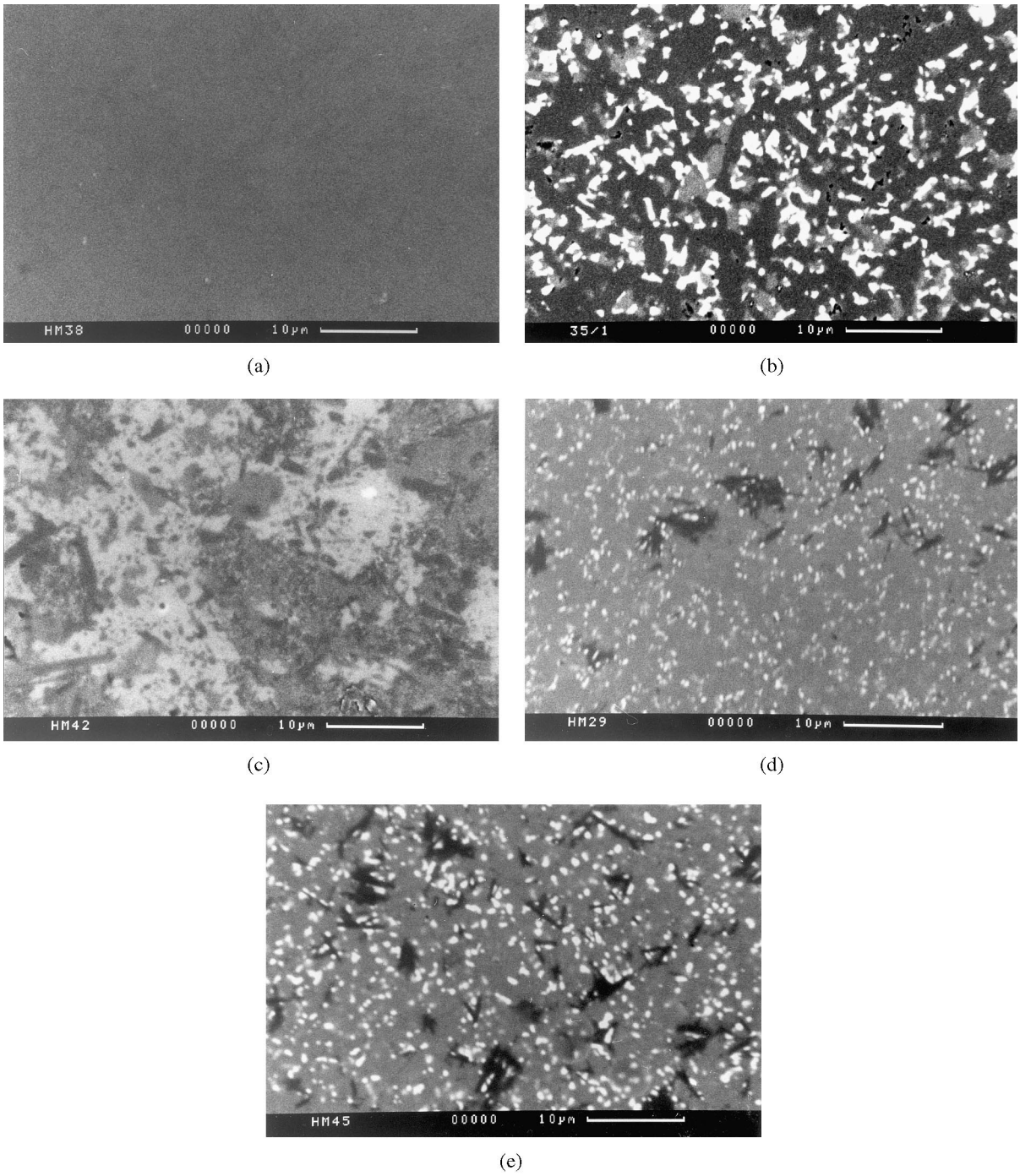

Fig. 3. Back-scattered SEM micrographs of the (a) CaO, (b) Nd_2O_3, (c) SrO, (d) Nd_2O_3-CaO, (e) Nd_2O_3– Yb_2O_3 samples after heat treatment at 1450°C for 168 h.

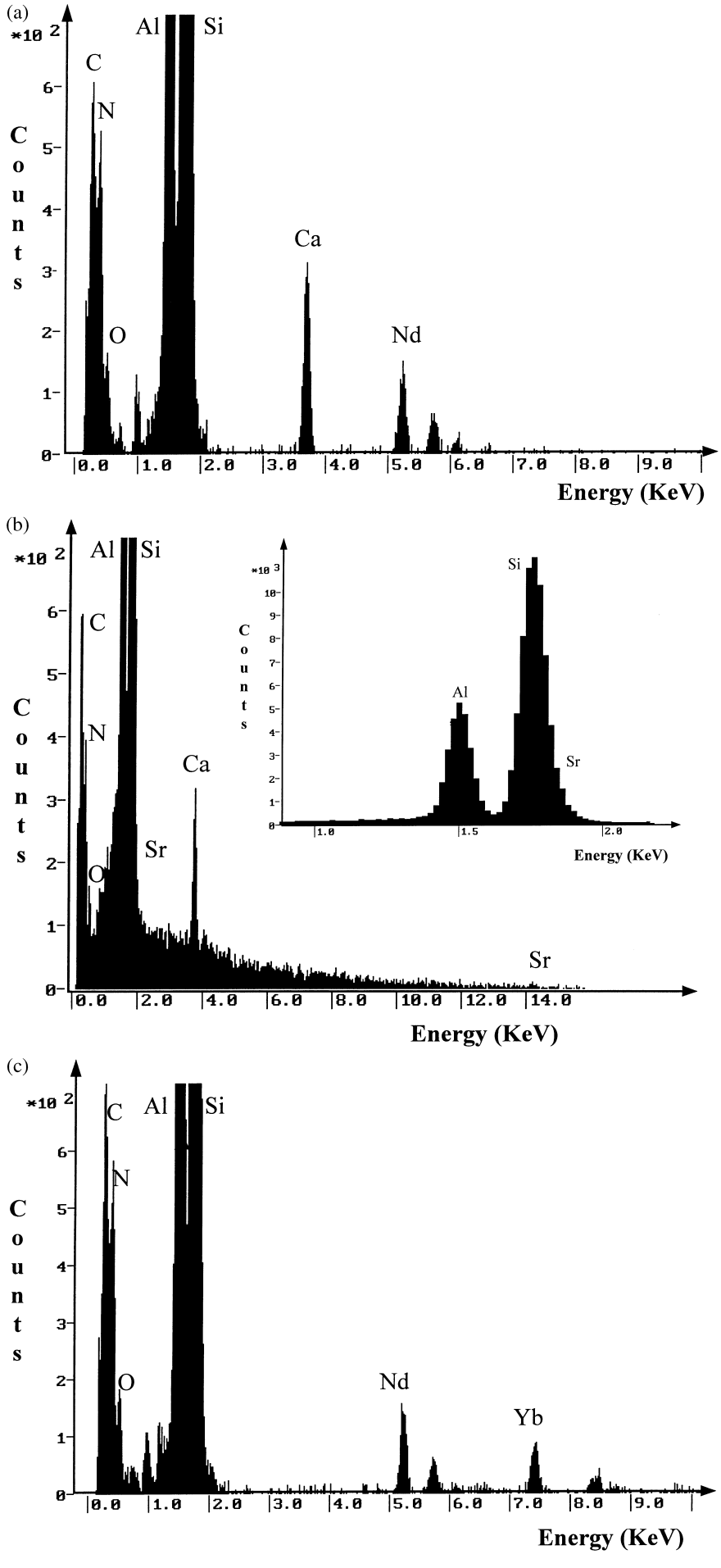

Fig. 4. EDX spectra of the α-sialon regions of (a) CaO– Nd_2O_3, (b) CaO–SrO, (c) $Yb_2O_3Nd_2O_3$ samples after heat treatment at 1450°C for 168 h.

the single-phase α-sialon phase-field in the calcium sialon system. Indeed, this may well be capable of being expressed more generally as a decrease in α-sialon stability with increasing valency of the interstitial cation, and would be consistent with recent work[19] on lithium α-sialons which shows that $x=2$ (i.e. $m=2$) materials can be readily prepared, and that n-values up to and in excess of 2·5 still give stable single-phase α-sialon products.

Extrinsic parameters varied (amount and composition of liquid phase, type of secondary crystalline phase, heat-treatment time, the presence or absence of β-sialon nucleation sites) all failed to induce $\alpha \rightarrow \beta$ transformation, showing that calcium α-sialon samples were thermodynamically stable under the conditions of these experiments. Moreover, variation of intrinsic (i.e. m and n) parameters) also failed to induce transformation, showing that the free energy versus temperature line for these calcium α-sialons must lie below that for β-sialon in the range 1450–1800°C.

An alternative way of understanding the present results is in terms of $\alpha \rightarrow \beta$ transformation temperature, $T_{\alpha\beta}$.[20] This concept has not been used significantly in previous studies, even though work on an $m=1{\cdot}5$, $n=1{\cdot}5$ Sm α-sialon composition showed $T_{\alpha\beta}$ to be ~1600°C.[21] Previous results are consistent in showing that the transformation temperature decreases with increasing atomic number in the rare earth α-sialon series, and in fact certain Yb α-sialon compositions are stable with respect to transformation, regardless of extrinsic variables showing that $T_{\alpha\beta}$ is so low, that regardless of thermodynamic considerations, kinetic factors prevent the reaction occurring. It must therefore be concluded from the present study that for all the calcium-containing α-sialons studied, the transformation temperature is below 1450°C. The results can be understood in terms of conventional phase diagram principles (i.e. a composition half way between the β-sialon line and the low m α-sialon limit would give equal amounts of the two phases). Moreover, it seems unlikely that calcium additions have a linear effect on transformation temperature, but rather that small additions give a significant reduction in transformation temperature, which with increasing Ca content may then gradually approach the appropriate value for a pure calcium a-sialon. A similar effect is observed for the stabilising influence of ytterbium on the much less stable neodymium α-sialon.

5 Conclusions

$\alpha \rightarrow \beta$ Sialon transformation has been explored in a wide range of single and double cation α-sialon ceramics in which calcium is the principal cation. In all cases $\alpha \rightarrow \beta$ transformation was not observed above 1450°C, and in mixed α-sialons, calcium acted as a stabiliser to inhibit transformation in α-sialon compositions which otherwise would have readily exhibited transformation. It is significant that even small amounts of calcium result in significant stabilization in these mixed cation materials.

The present results show that calcium α-sialons are significantly more stable than their rare earth counterparts, and this is consistent with the enhanced size of the single α-sialon phase field in the calcium sialon system, and the general trend of decreasing α-sialon stability with increasing valency of the interstitial cation. Furthermore, the $\alpha \rightarrow \beta$ transformation temperature for these materials must lie below the lowest heat-treatment temperature used in the present study (1450°C), and further work is needed below this temperature to see whether transformation can be induced under these conditions.

References

1. Ekström, T. and Ingelström, I., Characterization and properties of sialon ceramics. In Proceeding of the International Conference Non-oxide Technical and Engineering Ceramics, ed. S. Hampshire, Elsevier Applied Science; London, 1986, pp. 231–253.
2. Cao, G. Z., Metselaar, R. and Ziegler, G., Microstructure and properties of mixed $\alpha - \beta$ sialons. In 4th International Symposium on Ceramic Materials and Components for Engines, eds E. Carlsson, T. Johansson and L. Kahlman. Elsevier Applied Science; London, 1992, pp. 188–195.
3. Mandal, H., Thompson, D. P. and Ekstrom, T., Reversible $\alpha \rightarrow \beta$ SiAlON transformation in heat treated sialon ceramics. *J. Eur. Ceram. Soc.*, 1993, **12**, 421–429.
4. Mandal, H., Thompson, D. P. and Ekström, T., Optimization of sialon ceramics by heat treatment. In *Third Euro-Ceramics*, Vol. 3, eds P. Duran and J. F. Fernandez. Faenza Editrice Iberica S. L., Spain, 1993, pp. 385–390.
5. Ekström, T. and Shen, Z. J., Temperature stability of rare earth doped (α-sialon ceramics. In 5th *International Symposium on Ceramic Materials and Components for Engines*, eds D. S. Yan, X. R. Fu and S. X. Shi. World Sci. Publ. Co., 1995, pp. 206–210.
6. Mandal, H., Thompson, D. P. and Ekstrom, T., Mechanism for $\alpha \rightarrow \beta$ sialon transformation. In *Fourth Euro Ceramics*, Vol. 2, ed. C. Galassi. Gruppo Ed. Faenza Editrice, Italy, 1995, pp. 327–334.
7. Shen, Z., Ekström, T. and Nygren, M., Reactions occuring in post heat-treated α/β Sialons: on the thermal stability of α-Sialon. *J. Eur. Ceram. Soc.*, 1996, **16**, 873–883.
8. Zhao, R. and Cheng, Y.-B., Decomposition of Sm α-SiAlON phases during post-sintering heat treatment. *J. Eur. Ceram. Soc.*, 1996, **16**, 1001–1008.
9. Zhao, R., Cheng, Y.-B. and Drennan, J., Microstructural Features of the α to β-Sialon Phase Transformation. *J. Eur. Ceram. Soc.*, 1996, **12**, 529–534.
10. Mandal, H., Camuscu, N. and Thompson, D. P., Effect of starting composition, type of rare earth sintering additive and amount of liquid phase on $\alpha \rightarrow \beta$ sialon transformation. *J. Eur. Ceram. Soc.*, 1997, **17**, 599–613.
11. Mandal, H., Thompson, D. P., Liu, Q. and Gao, L., High temperature stability of α-sialon ceramics containing glass

additions. *Eur. J. Solid State. Inorg. Chem.*, 1997, **34**, 179–195.
12. Mandal, H. A., Thompson, D. P., The driving force for $\alpha \rightarrow \beta$ transformation in rare earth sialon ceramics. In *Fifth Euro Ceramics*, Vol. 2, eds P. Abelard, A. Autissier, A. Bouquillon, J. M. Haussonne, A. Mocellin, B. Raveau, F. Thevenot *Key Engineering Materials*, Vols 132–136, Switzerland, 1997, pp. 798–781
13. Falk, K. L. K., Shen, Z. and Ekström, T., Microstructural Stability of Duplex $\alpha-\beta$ Sialon Ceramics. *J. Eur. Ceram. Soc.*, 1997, **17**, 1099–1112.
14. Hewitt, C. L., Cheng, Y.-B., Muddle, B. C., Trigg, M. B., *J. Eur. Ceram. Soc.*, 1998, **18**, 417
15. Liddell, K., X-ray analysis of nitrogen ceramic phases. MSc thesis, University of Newcastle upon Tyne, UK, 1979.
16. Mandal, H., Camuscu, N. and Thompson, D.P., Comparison of the effectiveness of rare earth sintering additives on the high temperature sialon ceramics. *J. Mater. Sci.*, 1995, 30, 5901–5909.
17. Hwang, C. L, Susnitzky, D. W and Beaman, D. R., Preparation of multication α-sialon containing strontium. *J. Am. Ceram. Soc.*, 1995, **78**, 588–592.
18. Drew, R. A. L., Nitrogen glasses. Ph.D. thesis, University of Newcastle upon Tyne, UK, 1980.
19. Yu, Z., Thompson, D. R, and Bhatti, A. R., Preparation of single phase lithium α-sialons. *British Ceramic Transactions*, in press.
20. Mandal, H., Thompson D. P., Jack, K. H., $\alpha \rightleftharpoons \beta$ phase transformations in silicon nitride and sialons. In Proceedings of International Symposium on Novel Synthesis and Processing of Ceramics, October, 1997, in press.
21. Morand, C., Mandal, H. & Thompson, D.P., Evaluation of $\alpha \rightleftharpoons \beta$ sialon transformation temperatures for Ln-doped α-sialons. To be published.